

UCLA

UCLA Previously Published Works

Title

Azithromycin Protects against Zika virus Infection by Upregulating virus-induced Type I and III Interferon Responses.

Permalink

<https://escholarship.org/uc/item/01k8416c>

Journal

Antimicrobial Agents and Chemotherapy, 63(12)

ISSN

0066-4804

Authors

Li, Chunfeng
Zu, Shulong
Deng, Yong-Qiang
et al.

Publication Date

2019-12-01


DOI

10.1128/aac.00394-19

Peer reviewed



Azithromycin Protects against Zika Virus Infection by Upregulating Virus-Induced Type I and III Interferon Responses

Chunfeng Li,^{a,b,c,d} Shulong Zu,^{e,f} Yong-Qiang Deng,^c Dapei Li,^{a,b} Kislay Parvatiyar,^{g*} Natalie Quanquin,^g Jingzhe Shang,^{a,b} Nina Sun,^{e,f} Jiaqi Su,^{f,h} Zhenyang Liu,^{f,h} Min Wang,^{f,h} Saba R. Aliyari,^g Xiao-Feng Li,^c Aiping Wu,^{a,b} Feng Ma,^{a,b} Yi Shi,^{f,h} Karin Nielsen-Saines,ⁱ  Jae U. Jung,^j Frank Xiao-Feng Qin,^{a,b} Cheng-Feng Qin,^c Genhong Cheng^g

^aCenter of Systems Medicine, Institute of Basic Medical Sciences, Chinese Academy of Medical Sciences and Peking Union Medical College, Beijing, China

^bSuzhou Institute of Systems Medicine, Suzhou, Jiangsu, China

^cDepartment of Virology, State Key Laboratory of Pathogen and Biosecurity, Beijing Institute of Microbiology and Epidemiology, Beijing, China

^dInstitute for Immunity, Transplantation, and Infection, Stanford University, Stanford, California, USA

^eCAS Key Laboratory of Infection and Immunity, Institute of Biophysics, Chinese Academy of Sciences, Beijing, China

^fUniversity of Chinese Academy of Sciences, Beijing, China

^gDepartment of Microbiology, Immunology, and Molecular Genetics, University of California, Los Angeles, California, USA

^hCAS Key Laboratory of Pathogenic Microbiology and Immunology, Institute of Microbiology, Chinese Academy of Sciences, Beijing, China

ⁱDivision of Pediatric Infectious Diseases, Department of Pediatrics, David Geffen School of Medicine, UCLA, Los Angeles, California, USA

^jDepartment of Molecular Microbiology and Immunology, Keck School of Medicine, University of Southern California, Los Angeles, California, USA

ABSTRACT Azithromycin (AZM) is a widely used antibiotic, with additional antiviral and anti-inflammatory properties that remain poorly understood. Although Zika virus (ZIKV) poses a significant threat to global health, there are currently no vaccines or effective therapeutics against it. Here, we report that AZM effectively suppresses ZIKV infection *in vitro* by targeting a late stage in the viral life cycle. In addition, AZM upregulates the expression of host type I and III interferons and several of their downstream interferon-stimulated genes in response to ZIKV infection. In particular, we found that AZM upregulated the expression of MDA5 and RIG-I (pathogen recognition receptors induced by ZIKV infection) and increased the levels of phosphorylated TBK1 and IRF3. Interestingly, AZM treatment upregulated the phosphorylation of TBK1 without inducing the phosphorylation of IRF3 by itself. These findings highlight the potential use of AZM as a broad antiviral agent to combat viral infection and to prevent devastating ZIKV-associated clinical outcomes, such as congenital microcephaly.

KEYWORDS FDA-approved drug, azithromycin, Zika virus, type I and III interferon responses, antibiotics, antiviral agents, innate immunity, interferons

Although antibiotics are primarily used to combat bacterial infections by targeting critical microbial enzymes or structural components, some can also directly affect host cells. While this may lead to adverse effects such as bone marrow suppression, nonselective inhibition of monoamine oxidase, or damaging levels of reactive oxygen species that inhibit mitochondrial functions, some antibiotics have secondary effects that can actually be beneficial (1). Azithromycin (AZM) is a macrolide that was synthetically created in 1980 as an optimized form of the natural antibiotic erythromycin (2). The antibacterial mechanism of AZM is through the inhibition of protein synthesis by binding to the 50S subunit of bacterial ribosomes (3). However, AZM also has anti-inflammatory properties that make it particularly useful for treating infections with an inflammatory component and for controlling lung disease in cystic fibrosis patients (4). Interestingly, AZM has also been found to have antiviral properties (4–7). It was

Citation Li C, Zu S, Deng Y-Q, Li D, Parvatiyar K, Quanquin N, Shang J, Sun N, Su J, Liu Z, Wang M, Aliyari SR, Li X-F, Wu A, Ma F, Shi Y, Nielsen-Saines K, Jung JU, Qin FX-F, Qin C-F, Cheng G. 2019. Azithromycin protects against Zika virus infection by upregulating virus-induced type I and III interferon responses. *Antimicrob Agents Chemother* 63:e00394-19. <https://doi.org/10.1128/AAC.00394-19>.

Copyright © 2019 American Society for Microbiology. All Rights Reserved.

Address correspondence to Chunfeng Li, chunfeng@stanford.edu, Cheng-Feng Qin, qincf@bmi.ac.cn, or Genhong Cheng, gcheng@mednet.ucla.edu.

* Present address: Kislay Parvatiyar, Department of Microbiology and Immunology, Tulane University School of Medicine, New Orleans, Louisiana, USA.

Received 28 February 2019

Returned for modification 21 March 2019

Accepted 21 August 2019

Accepted manuscript posted online 16 September 2019

Published 21 November 2019

discovered that AZM, but not erythromycin or telithromycin, inhibited rhinoviruses by upregulating the type I interferon (IFN-I) responses in bronchial epithelial cells (5, 8). AZM was also found to inhibit cell entry by Ebola virus (EBOV), although the mechanism there remains unclear (6).

Zika virus (ZIKV) is a member of the *Flaviviridae* family, which can infect humans through mosquito vectors. The recent outbreaks of ZIKV that began on Yap Island in Micronesia in 2007 and spread to French Polynesia and across the Americas and the Caribbean region over the past decade revealed the first reported associations of infection with severe neurological conditions, including Guillain-Barré syndrome, meningoencephalitis, and congenital microcephaly (9–12). Direct evidence of ZIKV infection causing fetal growth restriction or congenital defects such as microcephaly was obtained using mouse models of *in utero* infection (13–15). ZIKV infection of neural progenitor cells in mice leads to apoptosis and inflammation, ultimately resulting in developmental defects of the fetal brain (13). Furthermore, it was demonstrated in male mice that ZIKV infection could cause testicular damage, leading to infertility (16, 17). ZIKV has become a global concern due to the rapidly expanding range of its mosquito vector, the international travel of asymptomatic carriers, and its ability to be sexually transmitted (18–22). It was also reported that ZIKV can be transmitted through close contact between guinea pigs (23). During the 2015–2016 ZIKV epidemic, there were millions of cases of ZIKV infection and about 3,000 confirmed cases of ZIKV congenital syndrome (24). Despite this, there are currently no approved vaccines or drugs to combat ZIKV infection or to treat its neurological sequelae. Consequently, there is an urgent need for anti-ZIKV therapeutics.

Interestingly, in addition to inhibiting rhinoviruses and EBOV, AZM was found to inhibit ZIKV infection in human glial cell lines (U87) and human astrocytes (7). However, the mechanism has not yet been studied (25, 26). AZM has additional advantages, such as being inexpensive and having an oral formulation that is effective over a short treatment course due to its persistence in tissues. For the aforementioned reasons, we decided that AZM merited further investigation as an anti-ZIKV agent.

IFN-I signaling by the innate immune system plays an essential role in inhibiting ZIKV infection, as demonstrated by the increased susceptibility of mice treated with immunosuppressors such as dexamethasone or lacking the IFN-I receptor (*Ifnar1*^{-/-} mice) (27–29). In addition, IFN-III_s, which are similar to IFN-I in expression and function (30, 31), were found to play an important role in combating ZIKV infection in human placental trophoblasts (32). The IFN family of cytokines exert their function through the induction of >300 IFN-stimulated genes (ISGs), whose products serve as antiviral factors or regulators of the immune response (33, 34). We showed that the ISG product 25-hydroxycholesterol (25HC) could inhibit ZIKV entry *in vitro* and ZIKV-associated microcephaly in a mouse model (35). Savidis et al. found that the ISG *IFITM3* could also inhibit ZIKV infection by blocking an early stage of the viral life cycle (36). Viperin and PARP12 suppress ZIKV replication by targeting ZIKV nonstructural (NS) proteins for degradation (37, 38). These results support using antiviral development strategies that upregulate the host's own natural immune defenses against ZIKV.

In the present study, we show that AZM upregulates the expression of pathogen recognition receptors (PRRs), IFN-I/III, and ISGs triggered by ZIKV and/or other viruses. Our results not only reveal the mechanism of AZM's activity against ZIKV but also strengthen its potential as a candidate for future clinical testing.

RESULTS

AZM inhibits ZIKV infection *in vitro*. In order to investigate the inhibitory effects of AZM on ZIKV infection *in vitro*, Vero cells were incubated with AZM for 12 h prior to ZIKV infection (GZ01 strain; multiplicity of infection [MOI] of 0.1). After 48 h of infection, ZIKV in the culture supernatant was quantified through quantitative reverse transcription-PCR (qRT-PCR) and plaque assays. Our analysis revealed that AZM inhibited ZIKV infection in a dose-dependent manner and that 6.59 μ M AZM inhibited infection by about 50% (Fig. 1A to C). We confirmed the results using immunofluorescence assays, which

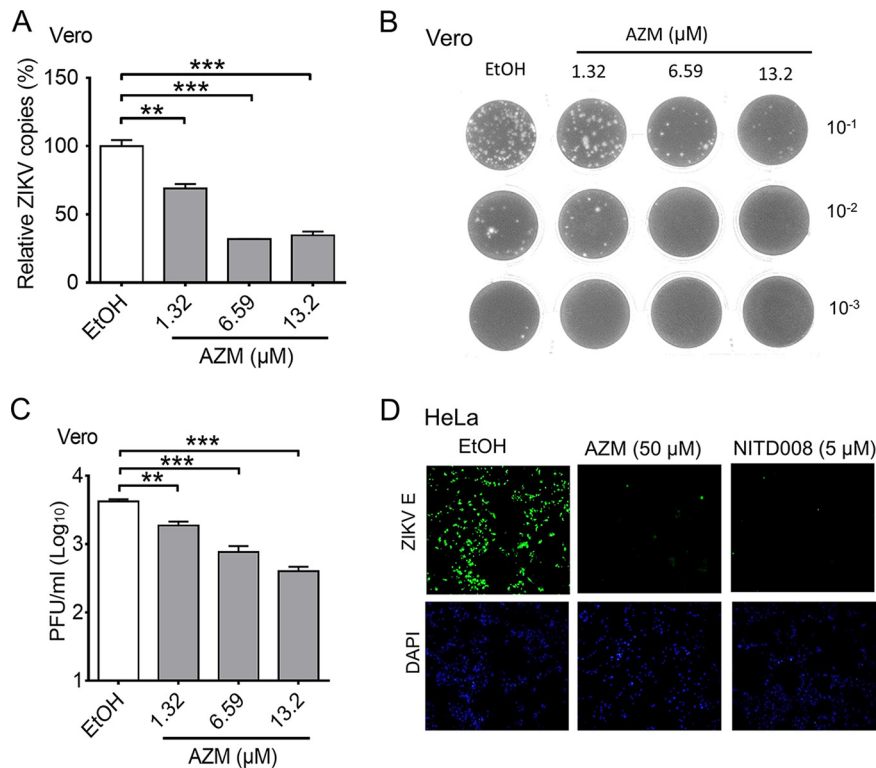


FIG 1 AZM inhibits ZIKV infection *in vitro*. EtOH or the indicated doses of AZM were used to treat Vero cells (A to C) or HeLa cells (D) for 12 h before infection with ZIKV (GZ01/2016 strain; MOI of 0.1). ZIKV in the culture supernatant was quantified by qRT-PCR (A) or plaque assays (B and C), and ZIKV in cells was detected by an immunofluorescence assay (D) at 48 hpi. Data in panels A and C are shown as mean \pm standard deviation. The relative numbers of ZIKV copies, compared to the negative control (EtOH-treated samples, set as 100%), are shown in panel A. Panels B and D are representative of two independent experiments. **, $P \leq 0.01$; ***, $P \leq 0.001$, one-way analysis of variance (ANOVA) followed by Dunnett's multiple-comparison test.

showed that 50 μM AZM could completely block the infection of HeLa cells with ZIKV (Fig. 1D), similar to 5 μM levels of the ZIKV polymerase inhibitor NITD008 (39). We further evaluated the inhibition by measuring the 50% inhibitory concentration (IC_{50}) values for AZM against the ZIKV GZ01 or FSS13025 strain in either A549 or Huh7 cells (Fig. 2A to C). The IC_{50} for the GZ01 strain in A549 cells was calculated to be 4.44 μM (Fig. 2A), and the IC_{50} s against GZ01 and FSS13025 in Huh7 cells were 4.97 and 1.23 μM , respectively (Fig. 2B and C). AZM could also inhibit dengue virus serotype 2 (DENV-2) replication in Vero cells, with an IC_{50} of 3.71 μM (Fig. 2D). Moreover, the 50% cytotoxic concentration (CC_{50}) values for AZM in Vero, HeLa, and Huh7 cells were 3.56 mM, 0.81 mM, and 1.36 mM, respectively (see Fig. S1A to C in the supplemental material), much higher than the IC_{50} s. These results demonstrate that AZM is a potent inhibitor of ZIKV *in vitro*, in agreement with previous findings (7).

AZM inhibits ZIKV infection at a late stage of the viral life cycle. To investigate the mechanism of action of AZM against ZIKV infection, we first performed a cell internalization assay (Fig. 3A). Our results revealed that AZM did not suppress ZIKV binding and/or entry (Fig. 3B). However, AZM inhibited ZIKV infection at a later stage of the viral life cycle (Fig. 3C). AZM also inhibited ZIKV (PRVABC59 strain) infection with a high MOI in HeLa cells at a late stage of viral replication (Fig. 3D). To examine whether ZIKV replication activity might be affected by AZM, a ZIKV replicon carrying the *Renilla* luciferase reporter was transcribed *in vitro* and transfected into BHK-21 cells. At 6 h posttransfection (hpt), the cells were treated with AZM at the indicated concentrations. As shown in Fig. 3E, AZM could suppress ZIKV replicon activity in a dose-dependent manner, although not as effectively as NITD008. Moreover, we showed that AZM could

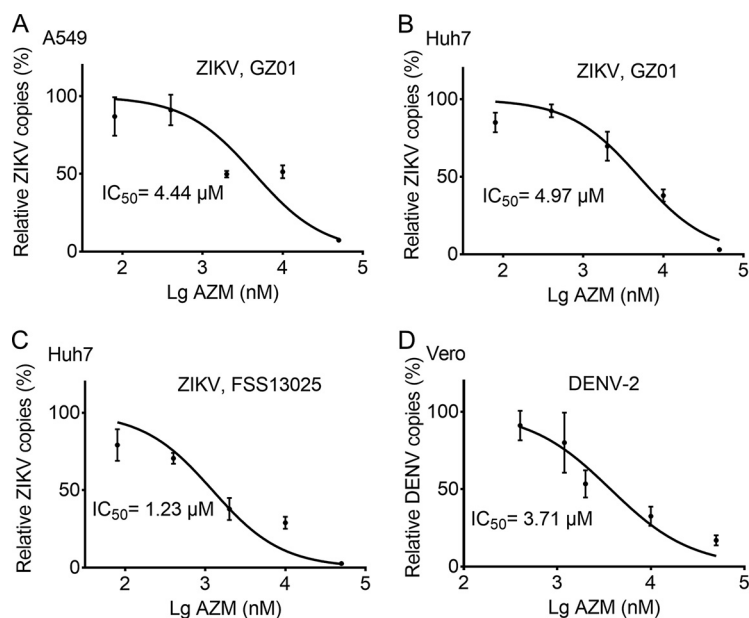


FIG 2 AZM broadly inhibits ZIKV replication *in vitro*. (A to C) Inhibitory effects of AZM on ZIKV GZ01 strain infection of A549 cells (A) or Huh7 cells (B) or on FSS13025 strain infection of Huh7 cells (C). The cells were pretreated with EtOH or the indicated dose of AZM for 12 h, followed by ZIKV infection (GZ01 or FSS13025 strain; MOI of 0.1) for 48 h. ZIKV RNA copies in the culture supernatants were quantified by qRT-PCR. The IC_{50} s of AZM on ZIKV infection are indicated. (D) Inhibitory effects of AZM on DENV-2 infection of Vero cells. Cells were pretreated with EtOH or AZM for 12 h, followed by DENV-2 infection (MOI of 0.01) for 24 h. DENV RNA copies in supernatants were quantified by qRT-PCR.

interfere with DENV replicon activity (Fig. 3F), suggesting that AZM might also effectively inhibit DENV infection, in agreement with the previous results (Fig. 2D). These findings were confirmed in Huh7 cells, where AZM could suppress ZIKV and DENV replicon activity effectively (Fig. S2A and B). However, using a ZIKV NS5 polymerase activity assay, we found that, unlike NITD008, AZM could not inhibit ZIKV NS5 polymerase activity *in vitro* (Fig. 3G), indicating AZM may targeting other ZIKV NS proteins related to RNA synthesis directly or indirectly. Therefore, our findings suggest that AZM blocks a late stage in the ZIKV life cycle.

AZM pretreatment enhances IFN-I/III responses after ZIKV infection. Given the known anti-inflammatory and antiviral properties of AZM in bronchial epithelial cells (5), we investigated whether AZM could enhance the natural IFN response to the virus. AZM is administered orally or given as an inhaled therapy against lung infection and for anti-inflammatory purposes in certain patients, such as those with cystic fibrosis (4). Because AZM is absorbed by epithelial cells of the lung and gastrointestinal tract, we selected the HT-29 human colon epithelial cell line and the A549 lung epithelial cell line for *in vitro* studies. HT-29 cells were pretreated with AZM 12 h before infection with ZIKV (GZ01 strain; MOI of 0.5). After 24 h, the ZIKV RNA levels were analyzed by qRT-PCR. AZM was found to inhibit ZIKV infection in HT-29 cells in a dose-dependent manner (Fig. 4A). Interestingly, we found that ZIKV infection induced the transcription of *IFNB* in HT-29 cells and its mRNA levels were further elevated by increasing doses of AZM (Fig. 4B). We also examined the mRNA levels of IFN-IIIs (interleukin-28 [IL-28] and IL-29), which play other important roles in the antiviral process (30, 31). Interestingly, we found that AZM also upregulated the mRNA expression of *IL-28* and *IL-29* during ZIKV infection (Fig. 4C and D).

We used transcriptome sequencing to evaluate the upregulated expression of genes associated with IFN-I and IFN-III-mediated immune responses during ZIKV infection. Interestingly, we found that pretreatment with AZM broadly enhanced this effect (Fig. 5A and B). Many of those genes are associated with antiviral functions, including *MX1*, *OAS1*, *IFITM3*, *ISG15*, and *TRIM22* (33, 34). More importantly, AZM also enhanced the

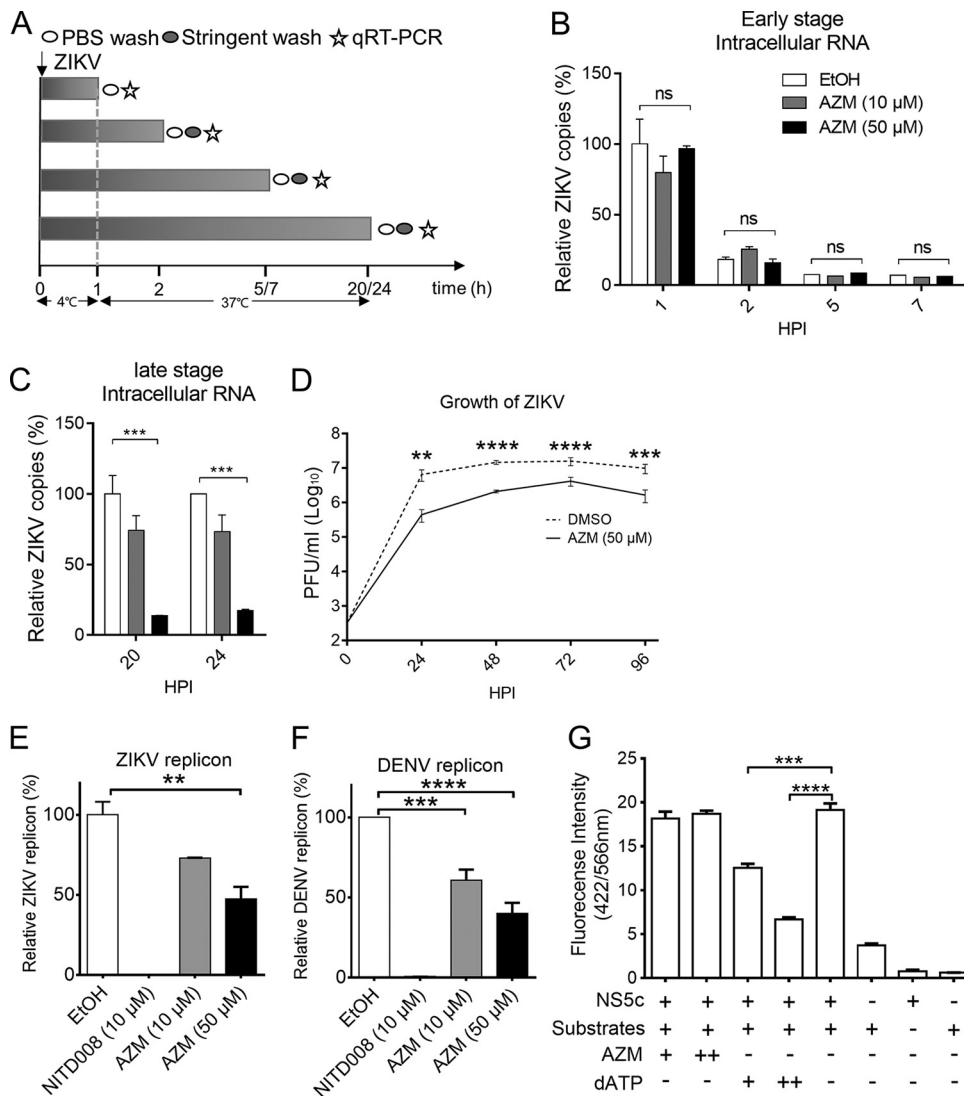


FIG 3 AZM blocks ZIKV replication at a late stage of viral infection. (A) Overview of our experimental design. BHK-21 cells were pretreated with either EtOH or AZM (10 or 50 μ M) for 12 h, followed by ZIKV infection (MOI of 1). (B and C) Quantification of intracellular RNA using qRT-PCR at the indicated hour postinfection (hpi). GAPDH was used for normalization. The numbers of ZIKV copies in EtOH-treated samples at 1 hpi (B) or 20 hpi (C) were set as 100%. ***, $P \leq 0.001$, two-way ANOVA followed by Dunnett's multiple-comparison test. ns, not significant. (D) Growth curves for ZIKV (PRVABC59 strain; MOI of 5) on Hela cells pretreated with DMSO or AZM. **, $P \leq 0.01$; ***, $P \leq 0.001$; ****, $P \leq 0.0001$, two-way ANOVA followed by Sidak's multiple-comparison test. (E and F) Effects of ASM on replicon RNA. BHK-21 cells were transfected with ZIKV (E) or DENV (F) replicon RNA. AZM was added to the cell medium at 6 hpi, and *Renilla* luciferase activity in cell lysates was determined at 48 hpi. NITD008 was used as a positive control. **, $P \leq 0.01$; ***, $P \leq 0.001$; ****, $P \leq 0.0001$, one-way ANOVA followed by Dunnett's multiple-comparison test. (G) Effects of AZM on ZIKV NS5 polymerase activity. The ZIKV NS5 RNA-dependent RNA polymerase domain (NS5c) was incubated with substrate (RNA template and BBT-ATP) and AZM or 2'-dATP (serving as a positive control). AZM/dATP +, 100 μ M; AZM/dATP ++, 500 μ M. Data in panels B and C are shown as mean \pm standard deviation. Panel E is representative of two independent experiments.

expression of *DDX58* (RIG-I) and *IFIH1* (MDA5) induced by ZIKV infection. These two PRRs have been found to play essential roles during flavivirus infection (40, 41). Gene ontology analysis confirmed that the genes upregulated by AZM largely function in host antiviral defense and the innate immune response, supporting the essential role of the innate immune system against ZIKV infection (Fig. 5C). qRT-PCR revealed that AZM treatment upregulated the expression of ISGs, including *MX1*, *CXCL10*, *TRIM22*, *RSAD2*, *OASL*, *IFITM3*, *CH25H*, and *ISG15*, in a dose-dependent manner after ZIKV infection (Fig. 6A to H). To expand our understanding of the mechanism by which AZM upregulates the expression of IFNs, we investigated the expression of different viral

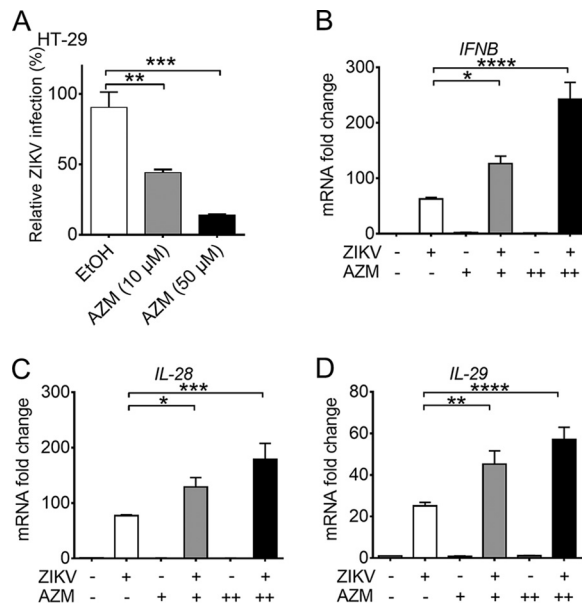


FIG 4 AZM enhances the expression of *IFNB*, *IL-28*, and *IL-29* in HT-29 cells after ZIKV infection. Human colon cancer epithelial cells (HT-29) were pretreated with AZM at the indicated concentrations for 12 h before infection with ZIKV (GZ01 strain; MOI of 0.5). qRT-PCR was used to quantify ZIKV RNA levels in the cell culture supernatant (A) and *IFNB* (B), *IL-28* (C), and *IL-29* (D) mRNA levels in HT-29 cells 24 hpi. *GAPDH* served as the housekeeping gene. AZM +, 10 μ M; AZM ++, 50 μ M. *, $P \leq 0.05$; **, $P \leq 0.01$; ***, $P \leq 0.001$; ****, $P \leq 0.0001$, one-way (A) or two-way (B to D) ANOVA followed by Dunnett's multiple-comparison test.

RNA sensors, including MDA5 (encoded by *IFIH1*) and RIG-I (encoded by *DDX58*), and the downstream DNA virus adaptor STING (encoded by *TMEM173*), which served as a negative control. Interestingly, the expression of *IFIH1* and *DDX58*, but not *TMEM173*, was enhanced by AZM after ZIKV infection (Fig. 7A to C). Although Toll-like receptors (TLRs) were found to play an important role in the induction of the antiviral immune responses to ZIKV and other flavivirus infections (42, 43), we found that *TLR2* and *TLR3* expression was not upregulated in AZM-pretreated cells after ZIKV infection (Fig. 7D and E). The expression of the reported ZIKV receptor AXL (42) was also not affected by AZM pretreatment after ZIKV infection (Fig. 7F).

Finally, we chose to examine whether the effects of AZM on the IFN-I/III responses to ZIKV infection could be reproduced in A549 cells. We found that, 24 h after treatment of A549 cells with AZM, the protein levels of PRRs such as MDA5 and RIG-I were upregulated in a dose-dependent manner, even though there was not much difference in ZIKV E protein expression levels (Fig. 8A). qRT-PCR results showed that *IFNB* mRNA levels were increased after the addition of 50 μ M AZM during ZIKV infection (data not shown). We also found that AZM pretreatment upregulated the protein levels of MX1, OAS1, STAT1, and phosphorylated versions of STAT1 (pS727 and pY701), in a dose-dependent manner, at 18 and 24 h postinfection (hpi) with ZIKV (GZ01 strain; MOI of 1) (Fig. 8B). To investigate whether AZM could enhance ISG expression induced by DNA viruses in A549 cells, we simulated an infection using poly(dA-dT) in the presence or absence of AZM. Through Western blot analysis, we found that AZM enhanced the expression of STAT1, MX1, and OAS1, in a dose-dependent manner, at 18 h poststimulation (Fig. 8C). We confirmed that AZM also could upregulate the expression of MX1 in HT-29 cells 24 h after DENV infection (Fig. 8D). Furthermore, we found that, while AZM treatment could enhance the expression of phosphorylated TBK1 (pTBK1) in human primary dermal fibroblasts, levels of pTBK1 expression were much higher after ZIKV infection (Fig. 8E). AZM-induced pTBK1 expression was also observed in A549 cells, but it was not enough to enhance the expression of phosphorylated IRF3 (pIRF3) without poly(dA-dT) (Fig.

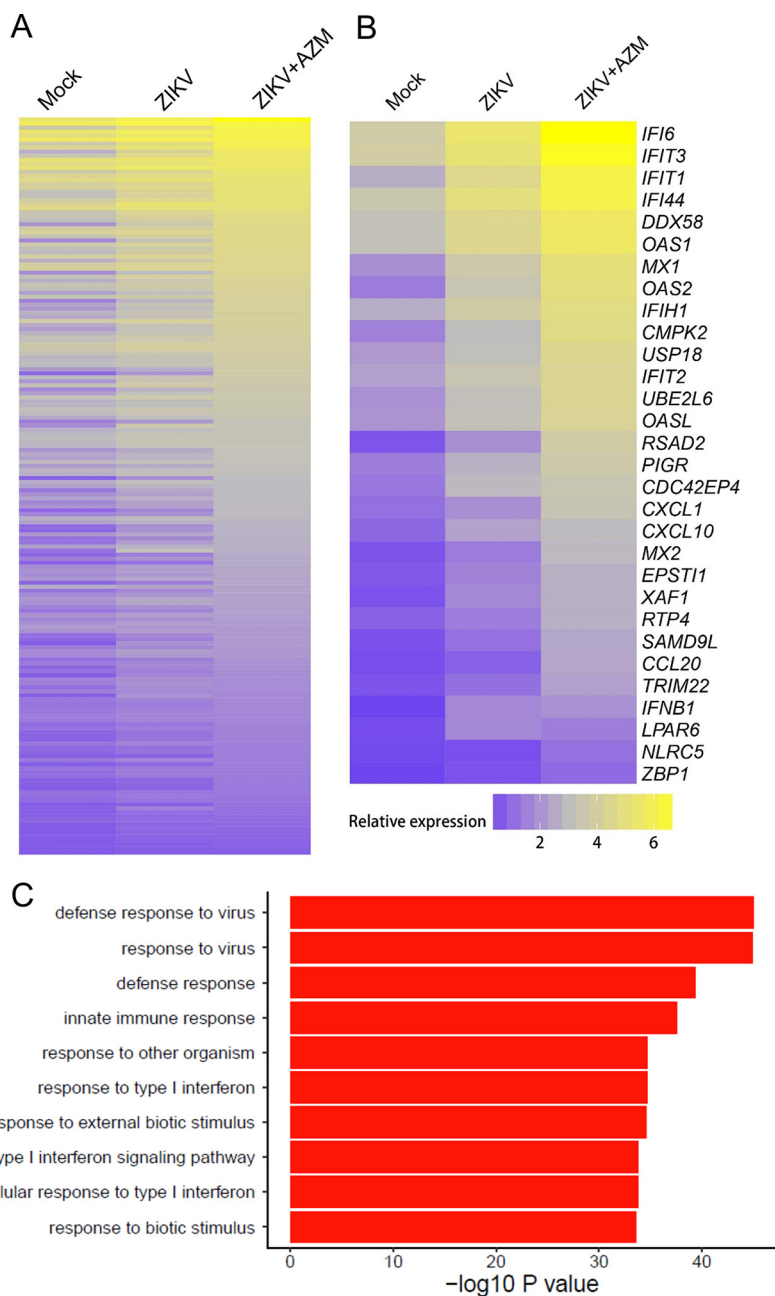


FIG 5 AZM broadly enhances the expression of ISGs in HT-29 cells after ZIKV infection. HT-29 cells were pretreated with EtOH or AZM (50 μ M) for 12 h and infected with ZIKV (MOI of 0.5). Gene expression profiles were analyzed by RNA sequencing at 24 hpi. (A) Heatmap showing relative expression of all upregulated antiviral genes. Two samples for each group were sequenced, and the means of the relative read numbers were compared to those for mock infection. Upregulation was defined as a fold change of >1.25 and a P value of <0.05 . (B) List of the 30 genes with the greatest upregulation. (C) Gene ontology analysis of all the upregulated genes. The data from two replicates are shown.

S3A and B). After ZIKV and poly(I-C) stimulation, AZM could further upregulate the expression of pIRF3 in RAW264.7 cells, in a dose-dependent manner (Fig. 8F and G). In agreement with these results, we noted antiviral effects induced by AZM in A549 cells against other viruses, including vesicular stomatitis virus and herpes simplex virus 1 (HSV-1), were not limited to ZIKV and DENV (Fig. S4A and B). Together, these results indicate that, in different cell types, AZM works as a broad antiviral reagent by upregulating the TBK1-pIRF3-IFN signaling axis.

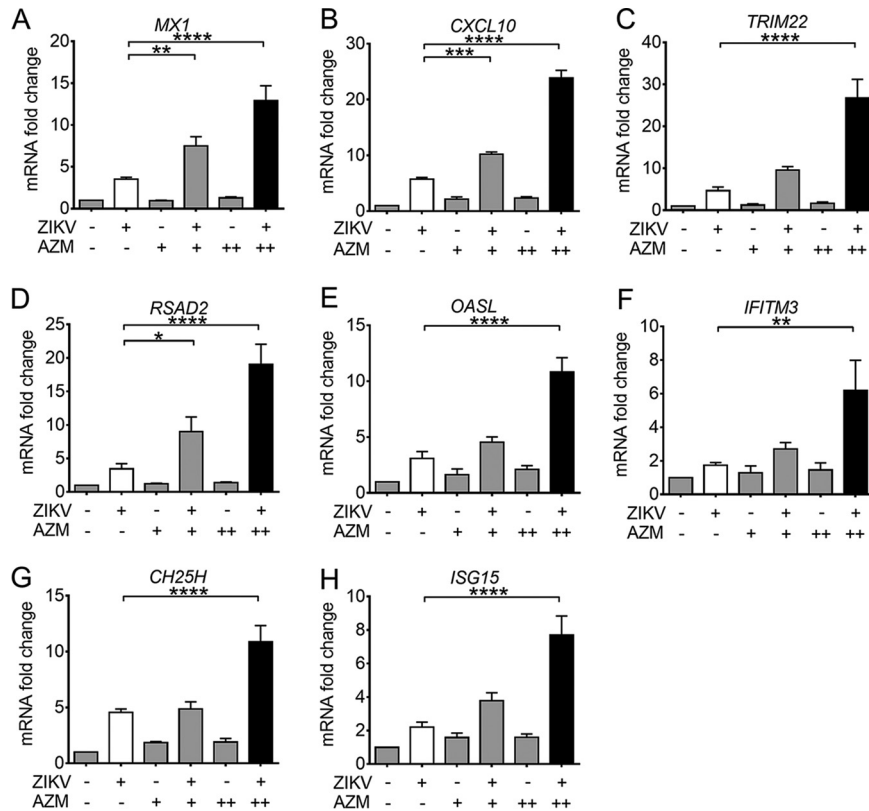


FIG 6 AZM upregulates ZIKV-induced ISG expression in HT-29 cells. HT-29 cells were pretreated with AZM as shown in Fig. 4, and *MX1* (A), *CXCL10* (B), *TRIM22* (C), *RSAD2* (D), *OASL* (E), *IFITM3* (F), *CH25H* (G), and *ISG15* (H) mRNA levels were analyzed by qRT-PCR at 24 hpi. *, $P \leq 0.05$; **, $P \leq 0.01$; ***, $P \leq 0.001$; ****, $P \leq 0.0001$, two-way ANOVA followed by Dunnett's multiple-comparison test.

DISCUSSION

Following the recent ZIKV outbreaks, much effort was placed in researching potential anti-ZIKV therapeutics. The most promising strategies included (but not were limited to) making use of natural antiviral immune activators and products (35), drug repurposing (44, 45), and *in silico* screening (46). In another study, our laboratory was able to show that 25HC, the enzymatic product of an ISG named *CH25H*, could effectively block ZIKV infection (35). In the current work, we reveal that AZM, an antibiotic with additional anti-inflammatory properties, can upregulate the host's natural IFN-I/III responses against ZIKV and suppress infection.

Recently, Retalack et al. published their finding that, of the 800 FDA-approved drugs they screened, AZM was among those that could inhibit ZIKV infection *in vitro* (7). Others also screened NIH collections or FDA-approved compounds to reveal that certain antibiotics, including nanchangmycin, daptomycin, and kitasmycin, had activity against ZIKV *in vitro* (45, 47, 48). However, their mechanisms of action against this virus remain largely unknown. In our study, we used both viral internalization and ZIKV replicon assays to demonstrate that AZM blocks ZIKV at a late stage of viral replication. In addition, AZM can enhance the expression of several ISGs, including *IFITM3*, *RSAD2*, and *MX1*, which have known anti-ZIKV functions (36, 37, 49). During the revision of our manuscript, Daniels et al. found that the nucleotide sensor ZBP1, which ranks in the top 30 genes upregulated by AZM after ZIKV infection, could suppress ZIKV infection by induction of the metabolite itaconate (50). Our results suggest that these other ISGs also merit further investigation for anti-ZIKV effects. Furthermore, we found that AZM could upregulate the expression of PRRs, including *IFIH1* and *DDX58*, which are also ISGs (34), indicating that AZM might enhance the sensitivity of host cells to viral infection through upregulation of the feedback loop of the IFN signaling cascade. Our

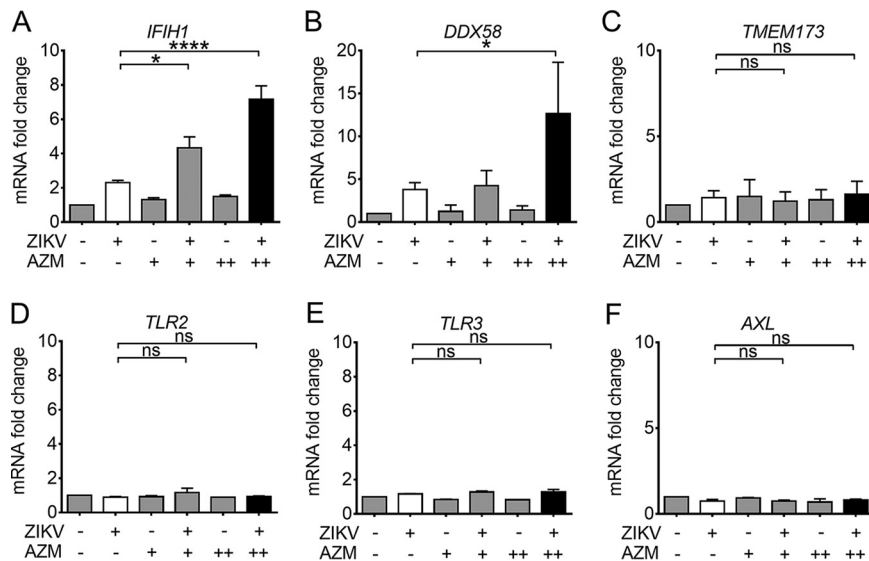


FIG 7 AZM enhances expression of viral RNA sensors in HT-29 cells after ZIKV infection. HT-29 cells were pretreated with AZM as shown in Fig. 4, and *IFIH1* (A), *DDX58* (B), *TMEM173* (C), *TLR2* (D), *TLR3* (E), and *AXL* (F) mRNA levels were analyzed by qRT-PCR at 24 hpi. *, $P \leq 0.05$; ****, $P \leq 0.0001$, two-way ANOVA followed by Dunnett's multiple-comparison test. ns, not significant.

data also showed that AZM alone could upregulate the phosphorylation of TBK1 without inducing the phosphorylation of IRF3 (see Fig. S3 in the supplemental material), suggesting that AZM might hold the PRR signaling pathway in a primed state by itself. After viral infection, the IFN signaling pathway was activated and upregulated. Schogler et al. found that AZM could inhibit rhinoviruses by upregulating the antiviral innate immune response mediated by MDA5, RIG-I, and TLR3 in cystic fibrosis airway epithelial cells and bronchial epithelial cells (4). The expression of TLR3 was not upregulated by AZM in our study, possibly due to the different cell types used; however, this could be further investigated.

We also demonstrated that AZM inhibited ZIKV replication in BHK-21 and Vero cells, which are deficient in IFN-I production (51, 52). Potential redundant roles of IFN-I and IFN-III might be a possible explanation for the observation that AZM could inhibit ZIKV infection in BHK-21 and Vero cells, since we found that AZM also could suppress ZIKV infection in *IFNAR1* knockout cells (Fig. S5). More interestingly, AZM could upregulate the expression of IL-29, IL-28, and CXCL10 in Vero cells after ZIKV infection (Fig. S6). This result is in agreement with findings that IFN- λ can be induced by virus infection in Vero cells (53) and can inhibit Dengue virus in Vero cells (54). We also noticed that the upregulation of ISGs by AZM in Vero cells was lower than that of IFN-IIIs after ZIKV infection, and we speculated that there are other mechanisms underlying the inhibitory function of AZM. Renna et al. showed that AZM could inhibit autophagy in macrophages (55). Given that autophagy plays an essential role during ZIKV replication (56, 57), exploring the effects of AZM on autophagy during ZIKV infection is another possible future direction for this work.

AZM is an FDA pregnancy category B drug, which means that animal reproduction studies have shown no adverse effects (58, 59). However, given that pregnant women are a significant target group for ZIKV treatment, the safety of using AZM during pregnancy would need to be studied more closely. Pharmacokinetic analyses indicate that, in humans, the recommended dosage of orally administered AZM yields concentrations of $\sim 2.8 \mu\text{M}$ in the placenta and 4 to $21 \mu\text{M}$ in fetal tissues and the adult brain (60–62). These concentrations are equal to or higher than the IC_{50} of AZM for ZIKV *in vitro*, indicating that this level of accumulation of AZM in fetal tissues, placenta, and brain should be sufficient to inhibit ZIKV replication.

In summary, our work not only demonstrates that AZM suppresses ZIKV infection

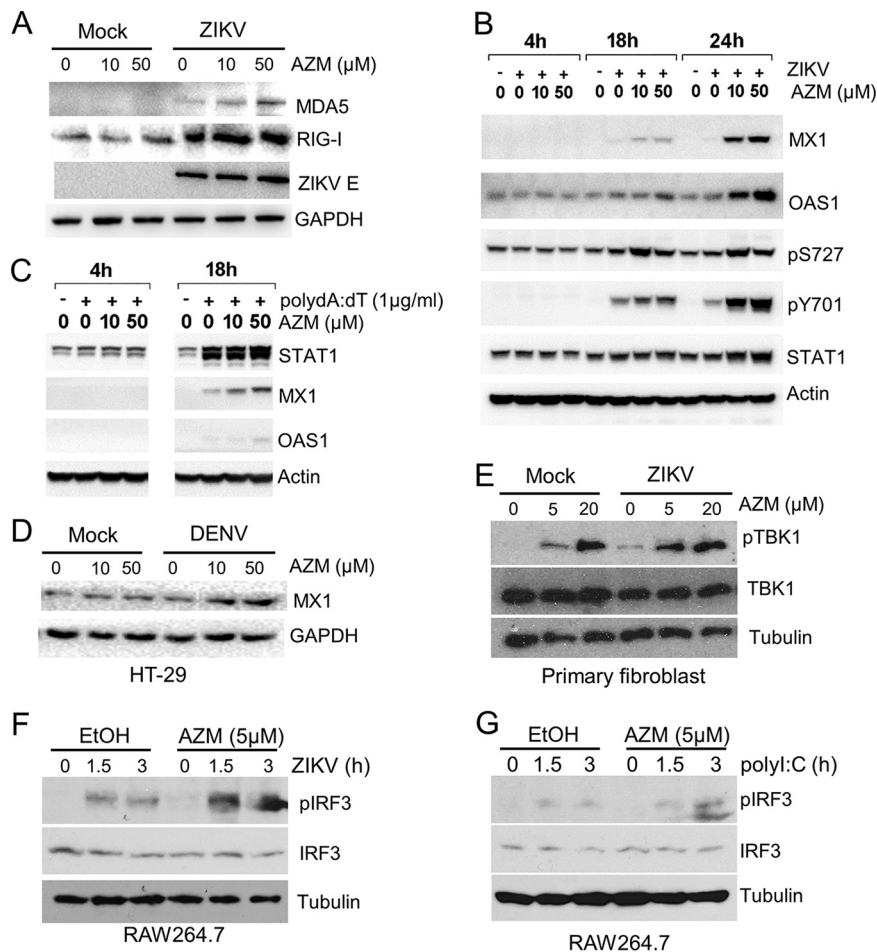


FIG 8 AZM upregulates the ZIKV-induced IFN response. (A to C) A549 cells were pretreated with the indicated doses of AZM or EtOH for 12 h and then infected with ZIKV (MOI of 1) (A and B) or stimulated with 1 $\mu\text{g}/\text{ml}$ poly(dA:dT) (C). Protein levels of RIG-I, MDA5, MX1, OAS1, STAT1 or its phosphorylated forms (pS727 and pY701), actin, and GAPDH were analyzed by Western blotting. (D to G) HT-29 cells (D), human primary fibroblasts (E), and RAW264.7 cells (F and G) were pretreated with the indicated doses of AZM or EtOH for 12 h and then stimulated with DENV-2 (D), ZIKV (E and F), or poly(I:C) (G) for 24 h (D), 3 h (E), or the indicated times (F and G). MX1, pTBK1, TBK1, pIRF3, IRF3, GAPDH, and tubulin protein levels were analyzed by Western blotting. The results are representative of two independent experiments.

effectively but also provides evidence of its mechanism of action. Given that AZM is already a well-studied and commonly used antibiotic and anti-inflammatory agent and is inexpensive and safe to use during pregnancy, there is sufficient reason for it to be pushed toward use in clinical trials to combat ZIKV infection and its associated diseases.

MATERIALS AND METHODS

Viruses, cells, and reagents. ZIKV strains (GZ01 [GenBank accession no. [KU820898](#)] and FSS13025/2010 [GenBank accession no. [JN860885](#)]) were described in our previous work (35). ZIKV strain PRVABC59 (GenBank [KU501215](#)) was kindly provided by Mehul Suthar (Emory University). HSV-1 expressing luciferase as a reporter (HSV-Luc) (63) was a gift from Chunfu Zheng. Cell lines were purchased from ATCC. A549, BHK-21, HeLa, Vero, and RAW264.7 cells were cultured in Dulbecco's modified Eagle's medium (DMEM) at 37°C in 5% CO₂, and HT-29 cells were cultured in F-12 medium at 37°C in 5% CO₂. Primary dermal fibroblasts (product no. PCS-201-012; ATCC) were cultured as suggested by ATCC. *IFNAR1*^{-/-} A549 cells were described previously (35). All viral stocks and cell lines used were free from mycoplasma contamination, as determined with a PCR-based detection kit (product no. J66117; Alfa Aesar). All media contained 10% fetal bovine serum (FBS) (ExCell Bio), 100 units/ml penicillin, and 50 $\mu\text{g}/\text{ml}$ streptomycin. Monoclonal antibody 4G2 was produced from hybridoma D1-4G2-4-15 (product no. HB-112; ATCC). NITD008 was a kind gift from Pei-Yong Shi (Novartis Institute for Infectious Diseases).

RNA isolation, reverse transcription, and real-time quantitative PCR. The assay was conducted as described previously (35). Briefly, total RNA was extracted with the Purelink RNA extraction kit (Thermo Fisher). ZIKV RNA copy numbers were measured by qRT-PCR with the PrimeScript One Step RT-PCR kit

TABLE 1 ISG, ZIKV, and DENV primers and probes used in this study

Gene	Forward primer	Reverse primer	Probe
<i>GAPDH</i>	GAACGGGAAGCTCACTGG	GCCTGCTTACCACCTTCT	
<i>IFNB</i>	ATGACCAACAAGTGTCTCCTCC	GGAATCCAAGCAAGTTGTAGCTC	
<i>IL-28</i>	CTGCCACATAGCCCAGTTCA	AGAAGCGACTCTTCTAAGGCATCTT	
<i>IL-29</i>	GGACGCCTTGAAGAGTCACT	AGAAGCCTCAGGTCCCAATTC	
<i>MX1</i>	GTTTCCGAAGTGACATCGCA	CTGCACAGTTGTTCTCAGC	
<i>CXCL10</i>	GTGGCATTCAAGGAGTACCTC	TGATGGCCTTCGATTCTGGATT	
<i>RSAD2</i>	CACAAAGAAGTGCCTGCTTGGT	AAGCGCATATATTTTCATCCAGAATAAG	
<i>OASL</i>	CTGATGCAGGAAGTATAGCAC	CACAGCGTCTAGCACCTCTT	
<i>TRIM22</i>	GGTTGAGGGGATCGTCAGTA	TTGGAAACAGATTTTGGCTTC	
<i>ISG15</i>	GAGAGGCAGCGAACTCATCT	CTTCAGCTCTGACACCGACA	
<i>IFITM3</i>	CATCCTCATGACCATTCTGC	TCAGTGATGCCTCCTGATCT	
<i>CH25H</i>	GCTGGCAACGAGTATATGAG	CGAGCAGTGTGACGTTTCATC	
<i>DDX58</i>	CTGGACCCTACCTACATCCTG	GGCATCCAAAAGCCACGG	
<i>IFIH1</i>	TCGAATGGGTATCCACAGACG	GTGGCGACTGCCTCTGAA	
<i>TMEM173</i>	CCAGAGCACACTCTCCGGTA	CGCATTGGGAGGGAGTAGTA	
<i>TLR2</i>	TTTCACTGCTTCAACTGGTA	TGGAGAGGCTGATGATGAC	
<i>TLR3</i>	AAATTAAGAGTTTTCTCCAGGGTGT	ATCCGAATGCTGTGTTTGC	
<i>AXL</i>	CCGTGGACCTACTCTGGCT	CCTTGGCGTTATGGGCTTC	
<i>ZIKV</i>	GGTCAGCGTCTCTAATAAACG	GCACCCTAGTGTCCACTTTTTCC	
<i>DENV-2</i>	CAGGCTATGGACACGTCACGAT	CCATYTGACAGCACCACATCTC	
<i>ZIKV</i>			FAM-AGCCATGACCGACACCACACCGT-BQ1 ^a
<i>DENV-2</i>			FAM-CTCYCCRAGAACGGGCTCGACTTCAA-BQ1

^aFAM, 6-carboxyfluorescein; BHQ1, black hole quencher 1.

(Takara, Beijing, China). SYBR green quantitative PCR mix (TransGen Biotech, Beijing, China) was used to quantify the ISG mRNA levels. The primers used in this study are listed in Table 1.

Plaque assay. BHK-21 cells were overnight cultured in a 12-well plate. Cells were washed once with phosphate-buffered saline (PBS) and infected with virus for 1 h at 37°C. The medium was then replaced with fresh DMEM containing 1% low-melting-point agarose and 2% FBS. Plaques were counted 4 days after infection.

Immunofluorescence assay. HeLa cells were treated with AZM for 12 h and then infected with ZIKV (MOI of 0.1) for 48 h. Cells were stained with 4',6-diamidino-2-phenylindole (DAPI) and 4G2 antibody, targeting the ZIKV E protein, to highlight the cell nucleus and ZIKV envelope, respectively.

Cell proliferation assay. The CellTiter 96 AQueous One Solution cell proliferation assay (product no. G3581; Promega) was used to test cell viability after AZM treatment. Briefly, cells were seeded overnight on a 96-well plate and then treated with AZM or dimethyl sulfoxide (DMSO) for 40 h. The One Solution reagent was added to the culture medium directly, and cells were incubated at 37°C for 1 h. The A_{490} was measured using a microplate reader. The A_{490} from samples treated with DMSO was set as 100%.

ZIKV internalization assay. A ZIKV internalization assay was performed as described previously (35). Briefly, BHK-21 cells were pretreated with AZM for 12 h and then infected with ZIKV (200 PFU/well or MOI of 1) at 4°C for 1 h. Cells were washed with cold PBS to remove unbound virus and then were incubated at 37°C for virus internalization. At the indicated time points, cells were washed once with PBS and treated with citric acid buffer (40 mM citric acid, 10 mM potassium chloride, 135 mM sodium chloride [pH 3.0]) for 1 min or with stringent buffer (1 M NaCl, 50 mM sodium bicarbonate [pH 9.5]) for 3 min to remove bound but not internalized viruses, as described previously (64). qRT-PCR was conducted to quantify intracellular RNA.

ZIKV and DENV replicon assays. The assays were performed as described previously (35, 65), with minor modifications. Briefly, ZIKV or DENV replicon plasmids composed of all ZIKV/DENV NS genes and a *Renilla* luciferase reporter gene were linearized, purified, and then transcribed *in vitro*. RNA was purified with the PureLink RNA extraction kit (Thermo Fisher), and 200 ng RNA/well was transfected with LIPO2000 (Thermo Fisher) into BHK-21 cells on a 24-well plate. At 6 hpt, AZM or ethanol (EtOH) was added to the cell culture. At 48 hpt, *Renilla* luciferase activity in cell lysates was measured with a GloMax-96 microplate luminometer. The luciferase activity in samples with EtOH was set to 100%.

In vitro RNA-dependent RNA polymerase activity assay of ZIKV NS5. The ZIKV NS5 RNA-dependent RNA polymerase domain (NS5c) was purified as described previously (66). A fluorescence-based alkaline phosphatase-coupled polymerase assay was used to detect the polymerase activity of ZIKV NS5c (67). Briefly, the RNA template (3'-untranslated region [UTR]-U_{30'}, synthesized by Sangon Biotech), ZIKV NS5c, and 2'-(2-benzothiazoyl)-6'-hydroxybenzothiazole-conjugated ATP (BBT-ATP) were resuspended in buffers consisting of 50 mM Tris-HCl (pH 7.5), 1 mM MnCl₂, or 0.001% Triton X-100, respectively, in diethyl pyrocarbonate (DEPC)-treated water. The RNA template solution was incubated at 58°C for 2 min and then placed at room temperature to allow the formation of the intramolecular hairpin. NS5c was mixed with the RNA template at 30°C for 30 min. The reaction was started by adding BBT-ATP and AZM. Polymerase activity was measured for 3 h at 30°C using 2 μM NS5c, 50 nM RNA, and 5 μM BBT-ATP in a 20-μl reaction mixture. Twenty microliters of stop buffer (200 mM NaCl, 25 mM MgCl₂, 1.5 M deoxyethanolamine) containing 25 nM calf intestinal alkaline phosphatase (CIP) (pH 10.0) was added to terminate the NS5c polymerase reaction and to allow hydrolysis of BBTpp_i by CIP. The BBT released was quantified after 1 h of incubation, and 2'-dATP was used as a positive control to validate the assay.

RNA sequencing. HT-29 cells were pretreated with AZM (50 μ M) or EtOH for 12 h. Cells were then infected with ZIKV (GZ01 strain; MOI of 0.5) or medium. Total RNA was extracted at 24 hpi. Library construction and sequencing were performed on the Illumina HiSeq X10 platform. Heatmaps were constructed with the DESeq2 R package. The negative binomial general linear model Wald test was used to test the significance of coefficients. In calculating the Wald test *P* values, the coefficients are scaled by their standard errors and then compared to a standard normal distribution. The results function without any arguments automatically performs a contrast of the last level of the last variable in the design formula over the first level. The contrast argument of the results function can be used to generate other comparisons.

Western blotting. Primary antibodies targeting human MDA5 (monoclonal antibody 5321), RIG-I (monoclonal antibody 4200), MX1 (monoclonal antibody 37849), OAS1 (monoclonal antibody 14498), pS727-STAT1 (monoclonal antibody 8826), pY701-STAT1 (monoclonal antibody 9167), STAT1 (monoclonal antibody 14994), TBK1 (monoclonal antibody 3504), pTBK1 (monoclonal antibody 5483), IRF3 (monoclonal antibody 4302), pIRF3 (monoclonal antibody 29047), β -actin (monoclonal antibody 3700), and tubulin (monoclonal antibody 5335) were purchased from Cell Signaling Technology. ZIKV E antibody (product no. GTX133314) was purchased from GeneTex. Glyceraldehyde-3-phosphate dehydrogenase (GAPDH) antibody was purchased from Kangwei Biotechnology (Beijing, China). Horseradish peroxidase-conjugated secondary antibody was used. The pictures were taken with a Bio-Rad imager (ChemiDoc MP imaging system).

Statistical analysis. Prism software (GraphPad) was used to analyze the data. All data are shown as mean \pm standard error of the mean from three repeat assays unless indicated otherwise.

Data availability. The raw sequence data reported in this article have been deposited in the Genome Sequence Archive (68) in the Beijing Institute of Genomics Data Center, Beijing Institute of Genomics, Chinese Academy of Sciences, under accession numbers CRA000783 and CRA000826 (publicly accessible at <http://bigd.big.ac.cn/gsa>).

SUPPLEMENTAL MATERIAL

Supplemental material for this article may be found at <https://doi.org/10.1128/AAC.00394-19>.

SUPPLEMENTAL FILE 1, PDF file, 0.3 MB.

ACKNOWLEDGMENTS

This work was supported by the National Natural Science Foundation of China (NSFC) (91542201, 81590765, 31670883, 31500145, 31870912, 81701567, 81773058, and 31800726). The Fundamental Research Funds for the Central Universities and PUMC Youth Fund (grant 3332016125) (C. Li), the CAMS Initiative for Innovative Medicine (grant 2016-I2M-1-005), the NIH (grants R01AI069120-06 and R01AI140718) (G. Cheng), the National Key Research and Development Project of China (grant 2016YFD0500304), the National Science and Technology Major Project of China (grant 2018ZX09711003), the NSFC Excellent Young Scientist Fund (grant 81522025), the Innovative Research Group (grant 81621005), the Newton Advanced Fellowship from the UK Academy of Medical Sciences, the NSFC (grant 81661130162) (C.-F. Qin), and Jiangsu Provincial Natural Science Foundation (BK20171232) (F. X.-F. Qin).

We thank Bali Pulendran, Mehul Suthar, Pei-Yong Shi, and Chunfu Zheng for providing reagents and all members of our team for helpful discussions.

C. Li, C.-F. Qin, and G. Cheng jointly directed the research. C. Li designed and performed most of the experiments and wrote the original draft of the manuscript. S. Zu, Y.-Q. Deng, D. Li, K. Parvatiyar, J. Shang, N. Sun, J. Su, Z. Liu, M. Wang, and S. R. Aliyari helped perform experiments. N. Quanquin, X.-F. Li, A. Wu, F. Ma, Y. Shi, K. Nielsevnsaines, J. U. Jung, and F. X.-F. Qin helped revise the manuscript or contributed reagents. All authors contributed to the writing.

REFERENCES

- Badal S, Her YF, Maher LJ, Ill. 2015. Nonantibiotic effects of fluoroquinolones in mammalian cells. *J Biol Chem* 290:22287–22297. <https://doi.org/10.1074/jbc.M115.671222>.
- Djokic S, Kobrehel G, Lazarevski G. 1987. Erythromycin series. XII. Antibacterial in vitro evaluation of 10-dihydro-10-deoxy-11-azaerythromycin A: synthesis and structure-activity relationship of its acyl derivatives. *J Antibiot (Tokyo)* 40:1006–1015. <https://doi.org/10.7164/antibiotics.40.1006>.
- Retsema J, Girard A, Schelkly W, Manousos M, Anderson M, Bright G, Borovoy R, Brennan L, Mason R. 1987. Spectrum and mode of action of azithromycin (CP-62,993), a new 15-membered-ring macrolide with improved potency against Gram-negative organisms. *Antimicrob Agents Chemother* 31:1939–1947. <https://doi.org/10.1128/aac.31.12.1939>.
- Schogler A, Kopf BS, Edwards MR, Johnston SL, Casaulta C, Kieninger E, Jung A, Moeller A, Geiser T, Regamey N, Alves MP. 2015. Novel antiviral properties of azithromycin in cystic fibrosis airway epithelial cells. *Eur Respir J* 45:428–439. <https://doi.org/10.1183/09031936.00102014>.
- Gielen V, Johnston SL, Edwards MR. 2010. Azithromycin induces antiviral responses in bronchial epithelial cells. *Eur Respir J* 36:646–654. <https://doi.org/10.1183/09031936.00095809>.
- Kouznetsova J, Sun W, Martinez-Romero C, Tawa G, Shinn P, Chen CZ,

- Schimmer A, Sanderson P, McKew JC, Zheng W, Garcia-Sastre A. 2014. Identification of 53 compounds that block Ebola virus-like particle entry via a repurposing screen of approved drugs. *Emerg Microbes Infect* 3:e84. <https://doi.org/10.1038/emi.2014.88>.
7. Retallack H, Di Lullo E, Arias C, Knopp KA, Laurie MT, Sandoval-Espinosa C, Mancía Leon WR, Krencik R, Ullian EM, Spatazza J, Pollen AA, Mandel-Brehm C, Nowakowski TJ, Kriegstein AR, DeRisi JL. 2016. Zika virus cell tropism in the developing human brain and inhibition by azithromycin. *Proc Natl Acad Sci U S A* 113:14408–14413. <https://doi.org/10.1073/pnas.1618029113>.
 8. Menzel M, Akbarshahi H, Tufvesson E, Persson C, Bjermer L, Uller L. 2017. Azithromycin augments rhinovirus-induced IFN β via cytosolic MDA5 in experimental models of asthma exacerbation. *Oncotarget* 8:31601–31611. <https://doi.org/10.18632/oncotarget.16364>.
 9. Carteaux G, Maquart M, Bedet A, Contou D, Brugieres P, Fourati S, Cleret de Langavant L, de Broucker T, Brun-Buisson C, Leparac-Goffart I, Mekontso Dessap A. 2016. Zika virus associated with meningoencephalitis. *N Engl J Med* 374:1595–1596. <https://doi.org/10.1056/NEJMc1602964>.
 10. Araujo LM, Ferreira ML, Nascimento OJ. 2016. Guillain-Barre syndrome associated with the Zika virus outbreak in Brazil. *Arq Neuropsiquiatr* 74:253–255. <https://doi.org/10.1590/0004-282X20160035>.
 11. Cao-Lormeau V-M, Blake A, Mons S, Lastère S, Roche C, Vanhomwegen J, Dub T, Baudouin L, Teissier A, Larre P, Vial A-L, Decam C, Choumet V, Halstead SK, Willison HJ, Musset L, Manuguerra J-C, Despres P, Fournier E, Mallet H-P, Musso D, Fontanet A, Neil J, Ghawché F. 2016. Guillain-Barre syndrome outbreak associated with Zika virus infection in French Polynesia: a case-control study. *Lancet* 387:1531–1539. [https://doi.org/10.1016/S0140-6736\(16\)00562-6](https://doi.org/10.1016/S0140-6736(16)00562-6).
 12. Brasil P, Pereira JP, Moreira ME, Ribeiro Nogueira RM, Damasceno L, Wakimoto M, Rabello RS, Valderramos SG, Halai U-A, Salles TS, Zin AA, Horovitz D, Daltro P, Boechat M, Raja Gabaglia C, Carvalho de Sequeira P, Pilotto JH, Medialdea-Carrera R, Cotrim da Cunha D, Abreu de Carvalho LM, Pone M, Machado Siqueira A, Calvet GA, Rodrigues Baiao AE, Neves ES, Nassar de Carvalho PR, Hasue RH, Marschik PB, Einspieler C, Janzen C, Cherry JD, Bispo de Filippis AM, Nielsen-Saines K. 2016. Zika virus infection in pregnant women in Rio de Janeiro: preliminary report. *N Engl J Med* 375:2321–2334. <https://doi.org/10.1056/NEJMoa1602412>.
 13. Li C, Xu D, Ye Q, Hong S, Jiang Y, Liu X, Zhang N, Shi L, Qin CF, Xu Z. 2016. Zika virus disrupts neural progenitor development and leads to microcephaly in mice. *Cell Stem Cell* 19:120–126. <https://doi.org/10.1016/j.stem.2016.04.017>.
 14. Cugola FR, Fernandes IR, Russo FB, Freitas BC, Dias JLM, Guimarães KP, Benazzato C, Almeida N, Pignatari GC, Romero S, Polonio CM, Cunha I, Freitas CL, Brandão WN, Rossato C, Andrade DG, Faria DdP, Garcez AT, Buchpiguel CA, Braconi CT, Mendes E, Sall AA, Zanotto PMdA, Peron JPS, Muotri AR, Beltrão-Braga PCB. 2016. The Brazilian Zika virus strain causes birth defects in experimental models. *Nature* 534:267–271. <https://doi.org/10.1038/nature18296>.
 15. Miner JJ, Cao B, Govero J, Smith AM, Fernandez E, Cabrera OH, Garber C, Noll M, Klein RS, Noguchi KK, Mysorekar IU, Diamond MS. 2016. Zika virus infection during pregnancy in mice causes placental damage and fetal demise. *Cell* 165:1081–1091. <https://doi.org/10.1016/j.cell.2016.05.008>.
 16. Ma W, Li S, Ma S, Jia L, Zhang F, Zhang Y, Zhang J, Wong G, Zhang S, Lu X, Liu M, Yan J, Li W, Qin C, Han D, Qin C, Wang N, Li X, Gao GF. 2016. Zika virus causes testis damage and leads to male infertility in mice. *Cell* 167:1511–1524.e1510. <https://doi.org/10.1016/j.cell.2016.11.016>.
 17. Govero J, Esakky P, Scheaffer SM, Fernandez E, Drury A, Platt DJ, Gorman MJ, Richner JM, Caine EA, Salazar V, Moley KH, Diamond MS. 2016. Zika virus infection damages the testes in mice. *Nature* 540:438–442. <https://doi.org/10.1038/nature20556>.
 18. D'Ortenzio E, Matheron S, Yazdanpanah Y, de Lamballerie X, Hubert B, Piorkowski G, Maquart M, Descamps D, Damond F, Leparac-Goffart I. 2016. Evidence of sexual transmission of Zika virus. *N Engl J Med* 374:2195–2198. <https://doi.org/10.1056/NEJMc1604449>.
 19. Driggers RW, Ho CY, Korhonen EM, Kuivanen S, Jaaskelainen AJ, Smura T, Rosenberg A, Hill DA, DeBiasi RL, Vezina G, Timofeev J, Rodriguez FJ, Levantov L, Razak J, Iyengar P, Hennenfent A, Kennedy R, Lanciotti R, Du Plessis A, Vapalahti O. 2016. Zika virus infection with prolonged maternal viremia and fetal brain abnormalities. *N Engl J Med* 374:2142–2151. <https://doi.org/10.1056/NEJMoa1601824>.
 20. Motta IJ, Spencer BR, Cordeiro da Silva SG, Arruda MB, Dobbin JA, Gonzaga YB, Arcuri IP, Tavares RC, Atta EH, Fernandes RF, Costa DA, Ribeiro LJ, Limonte F, Higa LM, Voloch CM, Brindeiro RM, Tanuri A, Ferreira OC, Jr. 2016. Evidence for transmission of Zika virus by platelet transfusion. *N Engl J Med* 375:1101–1103. <https://doi.org/10.1056/NEJMc1607262>.
 21. Musso D, Gubler DJ. 2016. Zika virus. *Clin Microbiol Rev* 29:487–524. <https://doi.org/10.1128/CMR.00072-15>.
 22. Rasmussen SA, Jamieson DJ, Honein MA, Petersen LR. 2016. Zika virus and birth defects: reviewing the evidence for causality. *N Engl J Med* 374:1981–1987. <https://doi.org/10.1056/NEJMs1604338>.
 23. Deng YQ, Zhang NN, Li XF, Wang YQ, Tian M, Qiu YF, Fan JW, Hao JN, Huang XY, Dong HL, Fan H, Wang YG, Zhang FC, Tong YG, Xu Z, Qin CF. 2017. Intranasal infection and contact transmission of Zika virus in guinea pigs. *Nat Commun* 8:1648. <https://doi.org/10.1038/s41467-017-01923-4>.
 24. Saiz JC, Martin-Acebes MA. 2017. The race to find antivirals for Zika virus. *Antimicrob Agents Chemother* 61:e00411-17. <https://doi.org/10.1128/AAC.00411-17>.
 25. Iannetta M, Ippolito G, Nicastri E. 2017. Azithromycin shows anti-Zika virus activity in human glial cells. *Antimicrob Agents Chemother* 61:e01152-17. <https://doi.org/10.1128/AAC.01152-17>.
 26. Saiz JC, Martin-Acebes MA. 2017. Reply to Iannetta et al., “Azithromycin shows anti-Zika virus activity in human glial cells.” *Antimicrob Agents Chemother* 61:e01192-17. <https://doi.org/10.1128/AAC.01192-17>.
 27. Dai L, Song J, Lu X, Deng YQ, Musyoki AM, Cheng H, Zhang Y, Yuan Y, Song H, Haywood J, Xiao H, Yan J, Shi Y, Qin CF, Qi J, Gao GF. 2016. Structures of the Zika virus envelope protein and its complex with a flavivirus broadly protective antibody. *Cell Host Microbe* 19:696–704. <https://doi.org/10.1016/j.chom.2016.04.013>.
 28. Lazear HM, Govero J, Smith AM, Platt DJ, Fernandez E, Miner JJ, Diamond MS. 2016. A mouse model of Zika virus pathogenesis. *Cell Host Microbe* 19:720–730. <https://doi.org/10.1016/j.chom.2016.03.010>.
 29. Chan JF, Zhang AJ, Chan CC, Yip CC, Mak WW, Zhu H, Poon VK, Tee KM, Zhu Z, Cai JP, Tsang JO, Chik KK, Yin F, Chan KH, Kok KH, Jin DY, Au-Yeung RK, Yuen KY. 2016. Zika virus infection in dexamethasone-immunosuppressed mice demonstrating disseminated infection with multi-organ involvement including orchitis effectively treated by recombinant type I interferons. *EBioMedicine* 14:112–122. <https://doi.org/10.1016/j.ebiom.2016.11.017>.
 30. Kottenko SV, Gallagher G, Baurin VV, Lewis-Antes A, Shen M, Shah NK, Langer JA, Sheikh F, Dickensheets H, Donnelly RP. 2003. IFN- λ s mediate antiviral protection through a distinct class II cytokine receptor complex. *Nat Immunol* 4:69–77. <https://doi.org/10.1038/ni875>.
 31. Sheppard A, Kindsvogel W, Xu W, Hendersson K, Schlutsmeyer S, Whitmore TE, Kuestner R, Garrigues U, Birks C, Roraback J, Ostrander C, Dong D, Shin J, Presnell S, Fox B, Haldeman B, Cooper E, Taft D, Gilbert T, Grant FJ, Tackett M, Krivan W, McKnight G, Clegg C, Foster D, Klucher KM. 2003. IL-28, IL-29 and their class II cytokine receptor IL-28R. *Nat Immunol* 4:63–68. <https://doi.org/10.1038/ni873>.
 32. Bayer A, Lennemann NJ, Ouyang Y, Bramley JC, Morosky S, Marques ET, Jr, Cherry S, Sadovsky Y, Coyne CB. 2016. Type III interferons produced by human placental trophoblasts confer protection against Zika virus infection. *Cell Host Microbe* 19:705–712. <https://doi.org/10.1016/j.chom.2016.03.008>.
 33. Schneider WM, Chevillotte MD, Rice CM. 2014. Interferon-stimulated genes: a complex web of host defenses. *Annu Rev Immunol* 32:513–545. <https://doi.org/10.1146/annurev-immunol-032713-120231>.
 34. Liu SY, Sanchez DJ, Aliyari R, Lu S, Cheng G. 2012. Systematic identification of type I and type II interferon-induced antiviral factors. *Proc Natl Acad Sci U S A* 109:4239–4244. <https://doi.org/10.1073/pnas.1114981109>.
 35. Li C, Deng YQ, Wang S, Ma F, Aliyari R, Huang XY, Zhang NN, Watanabe M, Dong HL, Liu P, Li XF, Ye Q, Tian M, Hong S, Fan J, Zhao H, Li L, Vishlaghi N, Buth JE, Au C, Liu Y, Lu N, Du P, Qin FX, Zhang B, Gong D, Dai X, Sun R, Novitsch BG, Xu Z, Qin CF, Cheng G. 2017. 25-Hydroxycholesterol protects host against Zika virus infection and its associated microcephaly in a mouse model. *Immunity* 46:446–456. <https://doi.org/10.1016/j.immuni.2017.02.012>.
 36. Savidis G, Perreira JM, Portmann JM, Meraner P, Guo Z, Green S, Brass AL. 2016. The IFITMs inhibit Zika virus replication. *Cell Rep* 15:2323–2330. <https://doi.org/10.1016/j.celrep.2016.05.074>.
 37. Panayiotou C, Lindqvist R, Kurhade C, Vonderstein K, Pasto J, Edlund K, Upadhyay AS, Overby AK. 2018. Viperin restricts Zika virus and tickborne encephalitis virus replication by targeting NS3 for proteasomal degradation. *J Virol* 92:e02054-17. <https://doi.org/10.1128/JVI.00501-18>.
 38. Li L, Zhao H, Liu P, Li C, Quanquin N, Ji X, Sun N, Du P, Qin CF, Lu N, Cheng G. 2018. PARP12 suppresses Zika virus infection through PARP-

- dependent degradation of NS1 and NS3 viral proteins. *Sci Signal* 11: eaas9332. <https://doi.org/10.1126/scisignal.aas9332>.
39. Deng YQ, Zhang NN, Li CF, Tian M, Hao JN, Xie XP, Shi PY, Qin CF. 2016. Adenosine analog NITD008 is a potent inhibitor of Zika virus. *Open Forum Infect Dis* 3:ofw175. <https://doi.org/10.1093/ofid/ofw175>.
 40. Kato H, Takeuchi O, Sato S, Yoneyama M, Yamamoto M, Matsui K, Uematsu S, Jung A, Kawai T, Ishii KJ, Yamaguchi O, Otsu K, Tsujimura T, Koh CS, Reis e Sousa C, Matsuura Y, Fujita T, Akira S. 2006. Differential roles of MDA5 and RIG-I helicases in the recognition of RNA viruses. *Nature* 441:101–105. <https://doi.org/10.1038/nature04734>.
 41. Loo YM, Fornek J, Crochet N, Bajwa G, Perwitasari O, Martinez-Sobrido L, Akira S, Gill MA, Garcia-Sastre A, Katze MG, Gale M, Jr. 2008. Distinct RIG-I and MDA5 signaling by RNA viruses in innate immunity. *J Virol* 82: 335–345. <https://doi.org/10.1128/JVI.01080-07>.
 42. Hamel R, Dejarnac O, Wichit S, Ekchariyawat P, Neyret A, Luplertlop N, Perera-Lecoin M, Surasombattapana P, Talignani L, Thomas F, Cao-Lormeau V-M, Choumet V, Briant L, Desprès P, Amara A, Yssel H, Missé D. 2015. Biology of Zika virus infection in human skin cells. *J Virol* 89:8880–8896. <https://doi.org/10.1128/JVI.00354-15>.
 43. Jensen S, Thomsen AR. 2012. Sensing of RNA viruses: a review of innate immune receptors involved in recognizing RNA virus invasion. *J Virol* 86:2900–2910. <https://doi.org/10.1128/JVI.05738-11>.
 44. Li C, Zhu X, Ji X, Quanqin N, Deng YQ, Tian M, Aliyari R, Zuo X, Yuan L, Afridi SK, Li XF, Jung JU, Nielsen-Saines K, Qin FX, Qin CF, Xu Z, Cheng G. 2017. Chloroquine, a FDA-approved drug, prevents Zika virus infection and its associated congenital microcephaly in mice. *EBioMedicine* 24:189–194. <https://doi.org/10.1016/j.ebiom.2017.09.034>.
 45. Barrows NJ, Campos RK, Powell ST, Prasanth KR, Schott-Lerner G, Soto-Acosta R, Galarza-Munoz G, McGrath EL, Urrabaz-Garza R, Gao J, Wu P, Menon R, Saade G, Fernandez-Salas I, Rossi SL, Vasilakis N, Routh A, Bradrick SS, Garcia-Blanco MA. 2016. A screen of FDA-approved drugs for inhibitors of Zika virus infection. *Cell Host Microbe* 20:259–270. <https://doi.org/10.1016/j.chom.2016.07.004>.
 46. Li C, Wang Z, Cao Y, Wang L, Ji J, Chen Z, Deng T, Jiang T, Cheng G, Qin FX. 2017. Screening for novel small-molecule inhibitors targeting the assembly of influenza virus polymerase complex by a bimolecular luminescence complementation-based reporter system. *J Virol* 91:e02282-16. <https://doi.org/10.1128/JVI.02282-16>.
 47. Adcock RS, Chu YK, Golden JE, Chung DH. 2017. Evaluation of anti-Zika virus activities of broad-spectrum antivirals and NIH clinical collection compounds using a cell-based, high-throughput screen assay. *Antiviral Res* 138:47–56. <https://doi.org/10.1016/j.antiviral.2016.11.018>.
 48. Rausch K, Hackett BA, Weinbren NL, Reeder SM, Sadovsky Y, Hunter CA, Schultz DC, Coyne CB, Cherry S. 2017. Screening bioactives reveals nanchangmycin as a broad spectrum antiviral active against Zika virus. *Cell Rep* 18:804–815. <https://doi.org/10.1016/j.celrep.2016.12.068>.
 49. Chen J, Liang Y, Yi P, Xu L, Hawkins HK, Rossi SL, Soong L, Cai J, Menon R, Sun J. 2017. Outcomes of congenital Zika disease depend on timing of infection and maternal-fetal interferon action. *Cell Rep* 21:1588–1599. <https://doi.org/10.1016/j.celrep.2017.10.059>.
 50. Daniels BP, Kofman SB, Smith JR, Norris GT, Snyder AG, Kolb JP, Gao X, Locasale JW, Martinez J, Gale M, Jr, Loo YM, Oberst A. 2019. The nucleotide sensor ZBP1 and kinase RPK3 induce the enzyme IRG1 to promote an antiviral metabolic state in neurons. *Immunity* 50: 64–76.e64. <https://doi.org/10.1016/j.immuni.2018.11.017>.
 51. Desmyter J, Melnick JL, Rawls WE. 1968. Defectiveness of interferon production and of rubella virus interference in a line of African green monkey kidney cells (Vero). *J Virol* 2:955–961.
 52. Liu WJ, Wang XJ, Clark DC, Lobigs M, Hall RA, Khromykh AA. 2006. A single amino acid substitution in the West Nile virus nonstructural protein NS2A disables its ability to inhibit alpha/beta interferon induction and attenuates virus virulence in mice. *J Virol* 80:2396–2404. <https://doi.org/10.1128/JVI.80.5.2396-2404.2006>.
 53. Prescott J, Hall P, Acuna-Retamar M, Ye C, Wathelot MG, Ebihara H, Feldmann H, Hjelle B. 2010. New World hantaviruses activate IFN α production in type I IFN-deficient Vero E6 cells. *PLoS One* 5:e11159. <https://doi.org/10.1371/journal.pone.0011159>.
 54. Palma-Ocampo HK, Flores-Alonso JC, Vallejo-Ruiz V, Reyes-Leyva J, Flores-Mendoza L, Herrera-Camacho I, Rosas-Murrieta NH, Santos-López G. 2015. Interferon lambda inhibits dengue virus replication in epithelial cells. *Virol J* 12:150. <https://doi.org/10.1186/s12985-015-0383-4>.
 55. Renna M, Schaffner C, Brown K, Shang S, Tamayo MH, Hegyi K, Grimsey NJ, Cusens D, Coulter S, Cooper J, Bowden AR, Newton SM, Kampmann B, Helm J, Jones A, Haworth CS, Basaraba RJ, DeGroot MA, Ordway DJ, Rubinsztein DC, Floto RA. 2011. Azithromycin blocks autophagy and may predispose cystic fibrosis patients to mycobacterial infection. *J Clin Invest* 121:3554–3563. <https://doi.org/10.1172/JCI46095>.
 56. Liang Q, Luo Z, Zeng J, Chen W, Foo SS, Lee SA, Ge J, Wang S, Goldman SA, Zlokovic BV, Zhao Z, Jung JU. 2016. Zika virus NS4A and NS4B proteins deregulate Akt-mTOR signaling in human fetal neural stem cells to inhibit neurogenesis and induce autophagy. *Cell Stem Cell* 19:663. <https://doi.org/10.1016/j.stem.2016.07.019>.
 57. Cao B, Parnell LA, Diamond MS, Mysorekar IU. 2017. Inhibition of autophagy limits vertical transmission of Zika virus in pregnant mice. *J Exp Med* 214:2303–2313. <https://doi.org/10.1084/jem.20170957>.
 58. Lin KJ, Mitchell AA, Yau W-P, Louik C, Hernández-Díaz S. 2013. Safety of macrolides during pregnancy. *Am J Obstet Gynecol* 208:221.e1–228. <https://doi.org/10.1016/j.ajog.2012.12.023>.
 59. Sarkar M, Woodland C, Koren G, Einarson AR. 2006. Pregnancy outcome following gestational exposure to azithromycin. *BMC Pregnancy Childbirth* 6:18. <https://doi.org/10.1186/1471-2393-6-18>.
 60. Jaruratanasirikul S, Hortiwakul R, Tantisarasart T, Phuenpathom N, Tusanasunthornwong S. 1996. Distribution of azithromycin into brain tissue, cerebrospinal fluid, and aqueous humor of the eye. *Antimicrob Agents Chemother* 40:825–826. <https://doi.org/10.1128/AAC.40.3.825>.
 61. Kemp MW, Miura Y, Payne MS, Jobe AH, Kallapur SG, Saito M, Stock SJ, Spiller OB, Ireland DJ, Yaegashi N, Clarke M, Hahne D, Rodger J, Keelan JA, Newnham JP. 2014. Maternal intravenous administration of azithromycin results in significant fetal uptake in a sheep model of second trimester pregnancy. *Antimicrob Agents Chemother* 58:6581–6591. <https://doi.org/10.1128/AAC.03721-14>.
 62. Sutton AL, Acosta EP, Larson KB, Kerstner-Wood CD, Tita AT, Biggio JR. 2015. Perinatal pharmacokinetics of azithromycin for cesarean prophylaxis. *Am J Obstet Gynecol* 212:812.e1–816. <https://doi.org/10.1016/j.ajog.2015.01.015>.
 63. Li Y, Wang S, Zhu H, Zheng C. 2011. Cloning of the herpes simplex virus type 1 genome as a novel luciferase-tagged infectious bacterial artificial chromosome. *Arch Virol* 156:2267–2272. <https://doi.org/10.1007/s00705-011-1094-9>.
 64. Fontes-Garfias CR, Shan C, Luo H, Muruato AE, Medeiros DBA, Mays E, Xie X, Zou J, Roundy CM, Wakamiya M, Rossi SL, Wang T, Weaver SC, Shi PY. 2017. Functional analysis of glycosylation of Zika virus envelope protein. *Cell Rep* 21:1180–1190. <https://doi.org/10.1016/j.celrep.2017.10.016>.
 65. Xie X, Zou J, Shan C, Yang Y, Kum DB, Dallmeier K, Neyts J, Shi PY. 2016. Zika virus replicons for drug discovery. *EBioMedicine* 12:156. <https://doi.org/10.1016/j.ebiom.2016.09.013>.
 66. Duan W, Song F, Wang H, Chai Y, Su C, Qi J, Shi Y, Gao GF. 2017. The crystal structure of Zika virus NS5 reveals conserved drug targets. *EMBO J* 36:919–933. <https://doi.org/10.15252/emboj.201696241>.
 67. Niyomrattanakit P, Abas SN, Lim CC, Beer D, Shi PY, Chen YL. 2011. A fluorescence-based alkaline phosphatase-coupled polymerase assay for identification of inhibitors of dengue virus RNA-dependent RNA polymerase. *J Biomol Screen* 16:201–210. <https://doi.org/10.1177/1087057110389323>.
 68. Wang Y, Song F, Zhu J, Zhang S, Yang Y, Chen T, Tang B, Dong L, Ding N, Zhang Q, Bai Z, Dong X, Chen H, Sun M, Zhai S, Sun Y, Yu L, Lan L, Xiao J, Fang X, Lei H, Zhang Z, Zhao W. 2017. GSA: Genome Sequence Archive. *Genomics Proteomics Bioinformatics* 15:14–18. <https://doi.org/10.1016/j.gpb.2017.01.001>.